Tuning the crystallographic, morphological, optical and electrical properties of ZnO:Al grown by spray pyrolysis.

Elisabetta Arca[a,*], Karsten Fleischer[a], Igor Shvets[a]

[a] Cleaner Energy Laboratory, CRANN, School of Physics, Trinity College Dublin, Ireland

[*]corresponding author:

Elisabetta Arca

School of Physics

CRANN Buildings, Room 2.26

Trinity College

Dublin 2

Rep. of Ireland

Ph: +353 (0)1 896 3808

Abstract

In this contribution the effect of different deposition conditions on the physical properties of ZnO:Al grown by spray pyrolysis is outlined. In particular, it will be shown that the solvent composition affects the crystallographic orientation of the deposited films, as well as their roughness and electrical properties. Using water leads to higher resistive films than methanol. The choice of precursor salts also has an effect on the electrical properties, as using organic precursors leads to lower resistivity films. In both cases post annealing helps to reduce the overall resistivity of the films. The reduction in resistivity will change depending on the initial deposition condition of the films, with lower values observed for films deposited at lower temperature. In optimum conditions a resistivity of 7×10^{-3} Ωcm can be reproducibly achieved with inexpensive air blast nozzles at atmospheric pressure.

Keywords: ZnO:Al; spray pyrolysis; electrical properties; crystal structure; post-annealing treatment

1. Introduction

Aluminated zinc oxide (ZnO:Al) is one of the most widely used n-type transparent conductive oxides (TCO). Its properties include high transparency in the visible range, good electrical conductivity and etching characteristics, in conjunction with the abundance, non-toxicity and relative low price of its constituents. This makes this oxide almost ideal for low cost, large scale TCO applications [1-6]. In particular for application in photovoltaic solar cells, ZnO:Al has the additional advantage of being easily texturized, thus enabling enhanced light trapping [7, 8]. The latter is crucial for indirect band gap absorbers in thin film cells (e.g. a-Si solar cells), to enhance the optical path length in the absorber and thus overall efficiency [9, 10]. On an industrial basis it is produced mostly by magnetron sputtering, which is a relatively expensive vacuum technique [5, 6]. Following growth, chemical etching is often performed in order to achieve the desired morphology and performance [9, 11]. For plasma-enhanced chemical vapor deposited ZnO:Al, the growth process itself leads to a textured film, useful for a solar cell front contact [12, 13]. Such texturing during growth can also be preferential for a low cost process such as spray pyrolysis. Previously, we reported the effect of the solvent on the structural and morphological properties of ZnO grown by spray pyrolysis [14]. In this contribution we extend the investigations to ZnO:Al. While boron dopaning (ZnO:B) is currently preferred for chemical vapor phase (CVD) grown ZnO due to better performance [15-17]; only few reports on spray pyrolysis grown ZnO:B have been published. These show no significantly different properties than ZnO:Al [18]. Hence, we focus on the more common Aluminum doping for the low cost spray pyrolysis process. In particular, we demonstrate tunability of haze values as a function of the solvent composition and discuss the electrical properties of the deposited film for different solvents and precursor salts. Finally, we discuss the effect of short post-annealing treatment in nitrogen environment for best performing films. Heat cycling in nitrogen has been previously investigated for films grown by magnetron sputtering [19, 20]. Depending on treatment time and temperatures the mechanism of improvement can vary from increased

crystallinity and mobility for high temperature, long time annealing [19] to modified grain boundaries for short low temperature annealing [20]. The latter procedure has been employed by us.

2. Experimental details

All ZnO:Al layers have been deposited by spray pyrolysis at atmospheric pressure using low cost air-blast nozzles on thin glass substrates (Roth, 24×60×0.2 mm). Nitrogen was used as carrier gas. Details of the home built apparatus have been previously reported [14]. For the deposition, zinc acetate, aluminum acetylacetonate (Al-$(ACAC)_3$), aluminum chloride ($AlCl_3$) and aluminum nitrate (Al-$(NO_3)_3$) were dissolved in water, methanol or a water/methanol mixture. As our main objective is the assessment of low cost material only inexpensive solvents and Aluminum precursors have been investigated. The optimum Zinc precursor was previously identified [14]. The concentration of salts was 0.2 M in zinc and typically 1.5 at.% of Al/Zn salt ratio. X-ray photoelectron spectroscopy (Omicron Multiprobe XP, monochromised Aluminum Kα source) was performed in order to confirm the actual Al content. A surface cleaning by Ar ion sputtering was employed to remove any residual precursor traces (10 min, 0.7 kV, 7 μA target current). As the optimum Al concentration of ~1.5% is difficult to measure, a linear relationship between precursor concentration and dopant incorporation for this system was confirmed in a previous study using similar precursors and higher concentrations [21, 22]. Within this work we therefore only refer to nominal concentrations in the precursor solution. The liquid flow was kept constant at 2.6 l/min. Nitrogen was used as carrier gas at a flow of 14 l/min. Deposition temperature was varied from 573K to 723K, with an optimum value found to be 683K for as grown films and 663K if films are post-annealed in nitrogen. Growth rates in spray pyrolysis are a complex function of substrate temperature, precursor molarity and solvent composition. For ZnO:Al growth in methanol they vary from 0.8 Å/s at 573 K to 7 Å/s at 673 K. Increasing the water to methanol ratio further increases growth rates up to 15 Å/s for growth in full water. For best comparison, growth times have been adapted to compare samples with similar thickness (500±100 nm) for all precursor solution compositions tested and several samples

have been measured for each composition. The thickness of each individual film was measured by spectrophotometry and cross sectional secondary electron microscopy (SEM). We compare films with an average thickness in the range given above. For water grown films there is an even larger variation within the film due to large droplets impacting the surfaces during growth. This leads to larger errors in the resistivity determination of these films. For the best performing films (methanol, 663-683 K) samples are grown for 10 min at a rate of ~7 Å/s.

For the crystallographic characterization, X-ray diffraction (XRD) was performed with a Bruker D8 Advance in θ/2θ geometry using Cu Kα radiation and a Ge(220) 2-bounce monochromator (Fig. 1). Scanning electron microscope (Zeiss Ultra) images were used to confirm crystal orientation (top view, 5 kV operating voltage, see Fig. 2) and film thickness (via cross sectional SEM, 2 kV operating voltage, not shown). Optical characterization was performed by spectrophotometry, using an integrating sphere (Perkin Elmer 650S). Both, total-integrated (T_T) and scattered-only transmission (T_S) measurements were performed in order to calculate haze values ($H=T_S/T_T$).

Electrical characterization was performed by 4 point probe measurements in linear configuration using gold plated, spring loaded contacts and a Keithley 2400 source meter. Carrier activation energies were determined by Arrhenius plots of the sheet resistance over a temperature range from 323 to 423 K. The same setup was used for the post-annealing treatments. In the latter case, the resistance system was evacuated and purged with clean nitrogen before starting the post-annealing treatment. The post-annealing treatments were carried out at 623 K in a nitrogen atmosphere at 10^5 Pa. The sheet resistance was monitored during the process, until a minimum value was reached. Typical post-annealing time was 5-10 minutes.

3. Results and discussion

Crystallographic properties of ZnO:Al grown using different solvent compositions (water, methanol and an equal mixture of them) and zinc acetate and aluminum chloride as precursors, were investigated by means of X-ray diffraction. According to the patterns (Figure 1), all films were single phase (Zincite, PDF n° 01-074-0534). Samples grown using water show randomly oriented crystals, while samples grown in methanol are highly oriented with the c-axis perpendicular to the surface.

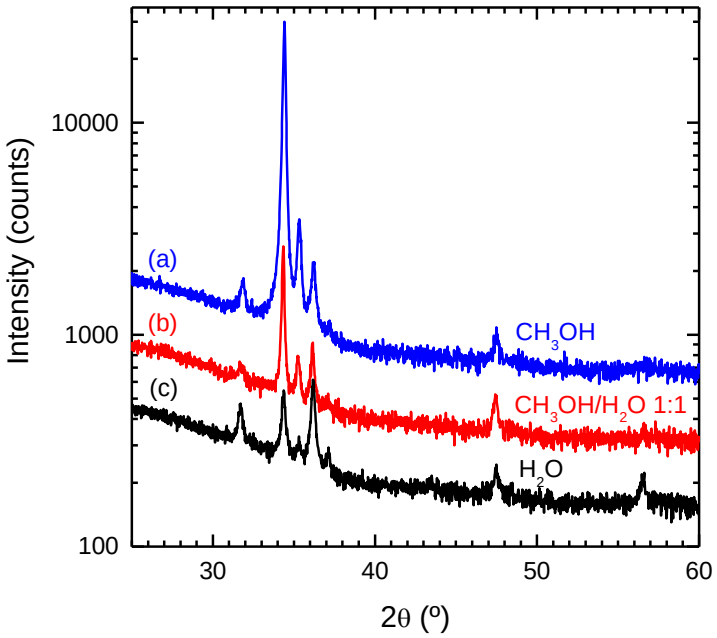

Figure 1: XRD patterns of ZnO:Al grown by using (a) only methanol, (b) methanol:water in 1:1 ratio, and (c) only water as solvent. It is worth noting that the methanol induces a high texturization of the film, while for water grown films randomly oriented crystallites are found. The average thickness of the particular films shown is 530±30, 410±20, and 400±100 nm respectively.

Top view SEM seen in Figure 2, confirmed the completely random orientation of facets in water grown films, while films grown in methanol show more regular columnar structure. At intermediate solvent composition few columnar hexagonal structures embedded in a randomly

oriented matrix are observed. These results are in agreement with the XRD data and further illustrate the importance of the solvent, previously reported for plain ZnO films [14].

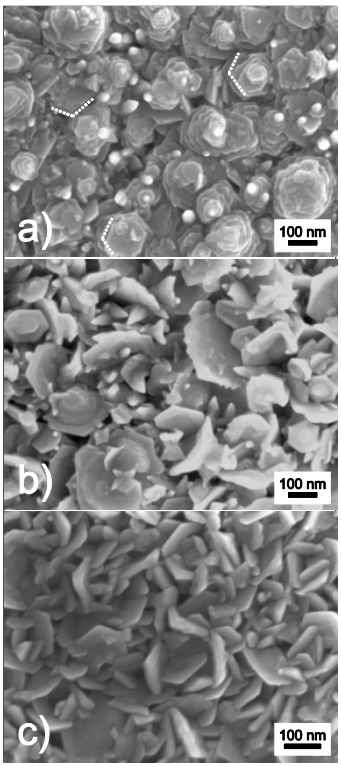

Figure 2: SEM images of the ZnO:Al films from Fig. 1 grown using (a) methanol, (b) methanol:water in 1:1 ratio, and (c) water. Indications of an underlying hexagonal structure can be seen for the sample grown with methanol as indicated by the presence of 120° angles. These structures progressively disappear as the water content in the solution is increased; instead hexagonal platelets occur in a random spatial orientation.

Figure 3 shows that the total transmittance is comparable for all films. However, the higher surface roughness for water grown films is clearly shown by the absence of Fabry-Perot thickness oscillations and a significant increase in the haze of the films.

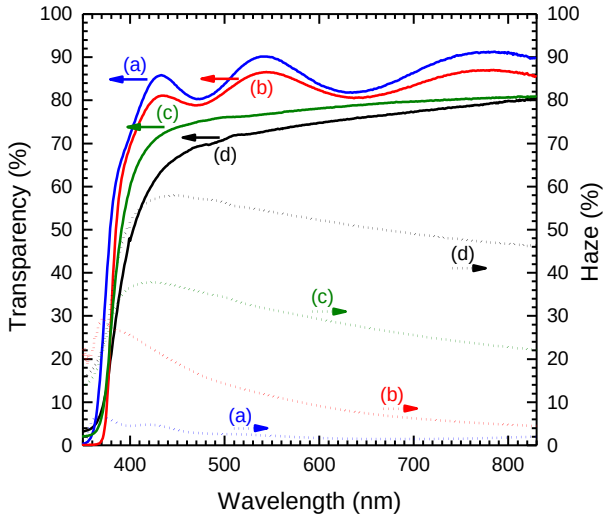

Figure 3: Total transmission of samples grown with (a) methanol, (b) water:methanol 1:2, (c) water:methanol 1:1, (d) water. The dotted curves are the spectroscopic haze values ($H=T_S/T_T$) of the same samples. The increased roughness of films using water suppresses the Fabry-Pérot oscillations and increases haze. For films (a) and (b), Fabry-Perot oscillations are still present and they lead to the conclusion that the two films have very similar thicknesses. Thus, in this case, the increase in the haze value is purely due to the change in the solvent composition. The thicknesses of the shown films are 520±20, 505±30, 550±100 nm and 400±100 nm respectively.

Finally, the electrical properties were investigated. In this case, different solvent and salts were used, as reported in Table 1, for both as deposited and post-annealed samples. Cross sectional SEM was performed in order to determine the thickness to calculate resistivity from the measured sheet resistance for each sample. The worst electrical performance was obtained for aluminum nitrate as a doping precursor. In this case, only a poor resistivity of 4 Ωcm was observed. When aluminum chloride was used in water, a higher resistivity was observed in comparison to the same precursor used in methanol. Both effects can be explained as a consequence of growing in oxygen rich conditions (water or oxidizing agent such as nitrate) as opposed to oxygen poor conditions (methanol). The additional burning of the organic solvents not only provides additional heat to the

growing film, but actively consumes oxygen in the process [14]. A further reduction in the resistivity is observed when an organic aluminum salt is used for doping.

Al precursor (1.5-2%)	**Solvent** Water:Methanol	ρ (Ωcm) as grown	ρ (Ωcm) annealed	**Haze** (%)	**T** (%)
Undoped	Methanol	$8(2) \times 10^{-2}$	$6(2) \times 10^{-2}$	2(1)	83(1)
Al-$(NO_3)_3$	Water	$4(1) \times 10^{0}$	$8(2) \times 10^{-2}$	39(5)	76(1)
$AlCl_3$	Water	$3(1) \times 10^{0}$	$3(2) \times 10^{-2}$	50(5)	74(1)
$AlCl_3$	1:1	$4(2) \times 10^{0}$	$5(2) \times 10^{-2}$	25(3)	79(2)
$AlCl_3$	Methanol	$10(2) \times 10^{-2}$	$2(1) \times 10^{-2}$	2(1)	83(1)
Al-$(ACAC)_3$	Methanol	$5(2) \times 10^{-2}$	$7(3) \times 10^{-3}$	1.5(1)	83(1)
Al-$(ACAC)_3$	1:2	1.3×10^{0}	$4(2) \times 10^{-2}$	8(2)	81(1)

Table 1: Summary of the average electrical properties of ZnO:Al films grown by using different solvents and salts. Both as deposited and post-annealed samples were characterized. Transmission and haze values are giving as spectral average in the visible range of 1.5-3 eV. Numbers in brackets denote the error based on variations between individual samples and local thickness variations within the samples.

As-deposited ZnO:Al layers grown by spray pyrolysis (but also sputtered films) can be improved significantly by post growth annealing in inert (N_2) atmospheres [19, 20]. The gain in resistivity however differs greatly between different doping salts and, more importantly, growth temperatures. Figure 4 shows an overview of sample resistivity before and after post-annealing in nitrogen at 623K.

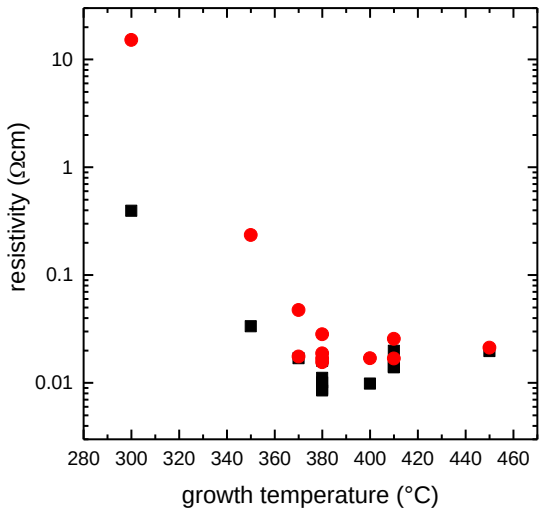

Figure 4: Resistivity of AZO films grown in methanol before (●) and after post-annealing in nitrogen (■) as a function of growth temperature. All samples were grown using Al-(ACAC)$_3$ as dopant with concentrations varying from 1-2 at%. Prior annealing samples with 2 at% give best resistivity, while post annealing films with 1.5 at% show a lower resistivity.

All films are grown in methanol using $AlCl_3$ and Al-$(ACAC)_3$ as doping precursors. It is obvious that post-annealing is more effective for films grown at low temperatures. The physical mechanism of the resistivity improvements is not fully understood. A combination of several key mechanisms can be responsible for the improvement, for example, the activation of an incorporated Al dopant via the removal of an adjacent compensating defect and/or the passivation of grain boundaries by N_2. Both these effects lead to a reduction in resistivity. As improvements for nominally undoped samples are only moderate (see Table 1), the activation of the Al dopant is the more likely scenario for our samples. Hydrogen is also suspected to play an important role in the conductivity of ZnO and annealing could potentially lead to a removal of interstitial hydrogen and hence an increase in resistivity. Indeed, at higher post-annealing temperatures (>673 K) we observed an increase in sheet resistance. To balance these two effects the sheet resistance was permanently monitored during annealing. The temperature was ramped up to 623 K (rate: 60 K/min) and the annealing was stopped as soon as the decrease in resistivity saturated or reversed.

Depending on sample thickness and initial growth temperature, the post annealing treatment continued for 5-10 min. In this case a minimum resistivity of 7×10^{-3} Ωcm was reached for films grown in methanol with 1.5 at% Al/Zn ratio using Al-$(ACAC)_3$. Thus, the resistivity of our sample is in line with those reported for spray pyrolysis grown films but higher than those reported for sputtered, or CVD deposited ZnO:Al. It is interesting to note that the ideal dopant concentration is affected by the post-annealing. While for as grown films the minimum resistivity was found at 2 at% Al/Zn ratio, for post annealed films it was only 1.5 at%. This highlights the complex nature of the resistivity of spray pyrolysis grown material.

While the resistivity of post-annealed spray pyrolysis grown ZnO:Al remains stable at room temperature for at least 6 months, care has been taken at elevated temperatures. During the post-annealing it was observed that if the nitrogen atmosphere is breached while the samples are still hot (>80K), an increase in resistivity was observed.

For a full comparison with other growth techniques Hall measurements have been performed for our best performing films. The bulk carrier concentration is about $1\text{-}2\times10^{19}$ cm^{-3} and the Hall mobility is 5-6 $cm^2V^{-1}s^{-1}$ [21]. It is worth noting that these films are not degenerated semiconductors, as the resistance vs. temperature measurements still show an effective carrier activation energy of about 5-6 meV. In comparison to films grown with more sophisticated techniques we have an overall higher mobility and higher carrier concentrations. It is reasonable to assume that the highly defective spray pyrolysis grown films have not just more grain boundaries limiting the carrier mobility but also more compensating defects preventing the formation extrinsic Al defects in an electrically active coordination. Indeed less than one in 100 incorporated Al atoms provide an active carrier in our films, illustrating the inherent limitations of a low cost technique such as spray pyrolysis.

While detrimental for the electrical properties, we have shown that by mixing water into the precursor solution the haze of as grown films can be significantly increased. While XRD data implies that the average grain size is not dramatically changed, SEM results clearly show a more

porous structure with more in-plane grain boundaries. In addition, the growth environment is more oxygen rich, leading to a reduction in the formation of the wanted n-type defects. Both effects together, lead to the dramatic increase in resistivity for water grown films.

4. Conclusion

Al:ZnO films were deposited by spray pyrolysis. It was demonstrated that the choice of solvent has a profound effect on the structural properties of the films. Using methanol leads to oriented films, while using water leads to randomly oriented, rough, and hazy films. These results were confirmed by top view SEM, showing hexagonal columnar structures in the former and random faceting in the latter case. This also affects the morphology and thus the macroscopic optical properties of the films. Thin films grown by using water are much rougher than those grown using methanol, and thus the former have a higher haze value. Both solvents and salts have an effect on the electrical properties of the films, with inorganic solvent and precursors leading to higher resistive samples in comparison to those grown by organic solvents and salts. Short post-annealing treatments lead to an improvement on the electrical properties in both cases. An overall minimum resistivity of 7×10^{-3} Ωcm can be achieved reproducibly by employing spray pyrolysis using simple air blast nozzles. For smooth films grown in methanol Al-$(ACAC)_3$ was found to be the best dopant, while for rougher, hazier films grown with methanol/water mixtures or water, $AlCl_3$ was the better dopant.

Acknowledgments

The authors would like to acknowledge financial support by Science Foundation Ireland under grant SFI 06/IN.1/I91 TIDA Feasibility 10.

[1] A. Janotti, C.G. Van de Walle, Reports on Progress in Physics 72 (2009) 126501.

[2] D.P. Norton, Y.W. Heo, M.P. Ivill, K. Ip, S.J. Pearton, M.F. Chisholm, T. Steiner, Materials Today 7 (2004) 34.

[3] U. Ozgur, Y.I. Alivov, C. Liu, A. Teke, M.A. Reshchikov, S. Dogan, V. Avrutin, S.J. Cho, H. Morkoc, J Appl Phys 98 (2005) 041301.

[4] S.J. Pearton, D.P. Norton, K. Ip, Y.W. Heo, T. Steiner, Progress in Materials Science 50 (2005) 293.

[5] A. Facchinetti, T.J. Marks, Transparent electronics From synthesis to application, Wiley, 2010.

[6] B. Szyszka, V. Sittinger, X. Jiang, R.J. Hong, W. Werner, A. Pflug, M. Ruske, A. Lopp, Thin Solid Films 442 (2003) 179.

[7] F. Ruske, C. Jacobs, V. Sittinger, B. Szyszka, W. Werner, Thin Solid Films 515 (2007) 8695.

[8] A. Campa, J. Krc, J. Malmstrom, M. Edoff, F. Smole, M. Topic, Thin Solid Films 515 (2007) 5968.

[9] J. Hupkes, B. Rech, O. Kluth, T. Repmann, B. Zwaygardt, J. Muller, R. Drese, M. Wuttig, Sol. Energ. Mat. Sol. Cells 90 (2006) 3054.

[10] V. Sittinger, F. Ruske, W. Werner, B. Szyszka, B. Rech, J. Hüpkes, G. Schöpe, H. Stiebig, Thin Solid Films 496 (2006) 16.

[11] O. Kluth, B. Rech, L. Houben, S. Wieder, G. Schöpe, C. Beneking, H. Wagner, A. Löffl, H.W. Schock, Thin Solid Films 351 (1999) 247.

[12] S. Nicolay, M. Despeisse, F.J. Haug, C. Ballif, Sol. Energ. Mat. Sol. Cells 95 (2011) 1031.

[13] J. Loffler, R. Groenen, J.L. Linden, M.C.M. van de Sanden, R.E.I. Schropp, Thin Solid Films 392 (2001) 315.

[14] E. Arca, K. Fleischer, I.V. Shvets, J Phys Chem C 113 (2009) 21074.

[15] J. Yin, H. Zhu, Y. Wang, Z. Wang, J. Gao, Y. Mai, Y. Ma, M. Wan, Y. Huang, Appl Surf Sci 259 (2012) 758.

[16] X.D. Zhang, Q. Huang, Y.F. Wang, Y. Liu, X.L. Chen, Y. Zhao, Thin Solid Films 520 (2011) 1186.

[17] S. Fay, J. Steinhauser, S. Nicolay, C. Ballif, Thin Solid Films 518 (2010) 2961.

[18] B.N. Pawar, S.R. Jadkar, M.G. Takwale, J Phys Chem Solids 66 (2005) 1779.

[19] F. Ruske, M. Roczen, K. Lee, M. Wimmer, S. Gall, J. Hüpkes, D. Hrunski, B. Rech, J Appl Phys 107 (2010) 013708.

[20] C. Lennon, R. Kodama, Y. Chang, S. Sivananthan, M. Deshpande, J Vac Sci Technol B 27 (2009) 1641.

[21] K. Fleischer, E. Arca, C. Smith, I.V. Shvets, Appl Phys Lett 101 (2012) 121918.

[22] K. Fleischer, E. Arca, I.V. Shvets, Sol. Energ. Mat. & Sol. C. 101 (2012) 262.